

Novel cysteine substitution p.(Cys1084Tyr) causes variable expressivity of qualitative and quantitative VWF defects

Orla Rawley,¹ Laura L. Swystun,¹ Christine Brown,¹ Kate Nesbitt,¹ Margaret Rand,² Taneya Hossain,² Robert Klaassen,³ Paula D. James,⁴ Manuel D. Carcao,² and David Lillicrap¹

¹Molecular Hemostasis Research Group, Department of Pathology and Molecular Medicine, Queen's University, Kingston, ON, Canada; ²Division of Hematology/Oncology, Department of Pediatrics, Hospital for Sick Children and University of Toronto, Toronto, ON, Canada; ³Department of Pediatrics, University of Ottawa, Ottawa, ON, Canada; and ⁴Department of Medicine, Queen's University, Kingston, ON, Canada

Key Points

- The p.(Cys1084Tyr) variant causes a variably expressed, complex, mixed phenotype form of von Willebrand disease.
- p.(Cys1084Tyr) VWF differentially associates with qualitative and/or quantitative defects in heterozygous and homozygous individuals.

von Willebrand factor (VWF) is an extremely cysteine-rich multimeric protein that is essential for maintaining normal hemostasis. The cysteine residues of VWF monomers form intra- and intermolecular disulfide bonds that regulate its structural conformation, multimer distribution, and ultimately its hemostatic activity. In this study, we investigated and characterized the molecular and pathogenic mechanisms through which a novel cysteine variant p.(Cys1084Tyr) causes an unusual, mixed phenotype form of von Willebrand disease (VWD). Phenotypic data including bleeding scores, laboratory values, VWF multimer distribution, and desmopressin response kinetics were investigated in 5 members (2 parents and 3 daughters) of a consanguineous family. VWF synthesis and secretion were also assessed in a heterologous expression system and in a transient transgenic mouse model. Heterozygosity for p.(Cys1084Tyr) was associated with variable expressivity of qualitative VWF defects. Heterozygous individuals had reduced VWF:GPIbM (<0.40 IU/mL) and VWF:CB (<0.35 IU/mL), as well as relative reductions in high-molecular-weight multimers, consistent with type 2A VWD. In addition to these qualitative defects, homozygous individuals also displayed reduced factor VIII (FVIII):C/VWF:Ag, leading to very low FVIII levels (0.03-0.1 IU/mL) and reduced VWF:Ag (<0.40 IU/mL) and VWF:GPIbM (<0.30 IU/mL). Accelerated VWF clearance and impaired VWF secretion contributed to the fully expressed homozygous phenotype with impaired secretion arising because of disordered disulfide connectivity.

Introduction

The basic von Willebrand factor (VWF) functional unit, the monomer, exhibits considerable internal homology and is composed of a series of repeated domains stabilized by extensive intramolecular disulfide bonding.¹ Highly conserved cysteine residues are dispersed throughout the VWF sequence but cluster mainly in the N and C termini, where they participate in intermolecular disulfide interactions that are essential for the formation of high-molecular-weight multimers (HMWM). VWF monomers become disulfide-linked at the C terminus within the endoplasmic reticulum (ER) to form VWF dimers that are in turn disulfide linked to form HMWM as they pass through the Golgi apparatus and are packaged into Weibel Palade bodies (WPBs) for secretion. Previously, it was suggested that initial pairing of all

Submitted 11 August 2021; accepted 23 November 2021; prepublished online on *Blood Advances* First Edition 12 January 2022; final version published online 9 May 2022. DOI 10.1182/bloodadvances.2021005928.

Sequencing data can be found in GenBank (ncbi.nlm.nih.gov/genbank, accession numbers OM169364, OM169365, and OM169366). All original data and protocols can be made available to other investigators upon request by contacting the corresponding author at orla.rawley@queensu.ca.

The full-text version of this article contains a data supplement.

© 2022 by The American Society of Hematology. Licensed under Creative Commons Attribution-NonCommercial-NoDerivatives 4.0 International (CC BY-NC-ND 4.0), permitting only noncommercial, nonderivative use with attribution. All other rights reserved.

cysteines is critical to ensure correct VWF folding during the initial stages of synthesis. However, a proportion of plasma-derived and recombinant VWF molecules have been reported to contain unpaired cysteine residues.²⁻⁵

Cysteine residues and their associated disulfide bonds are critical for maintaining VWF structure and function, and the functional roles of several VWF disulfide bonds have been defined. In particular, long-range intramolecular disulfides in the VWF A1 and A3 domains, as well as a rare vicinal disulfide between p.(Cys1669) and p.(Cys1670) in the A2 domain, play key roles in regulating the hemostatic activity and proteolytic processing of VWF.⁶⁻⁸

Cysteine variants account for ~5% of all pathogenic VWF variants and are typically associated with highly penetrant forms of von Willebrand disease (VWD).⁹⁻¹¹ Interestingly, accumulating evidence suggests that cysteine variants are associated with complex VWD phenotypes. For example, well-characterized cysteine variants p.(Cys1130Phe) and p.(Cys1149Arg) exert dominant-negative effects on VWF secretion, cause accelerated VWF clearance, and lead to aberrant multimerization resulting in overlapping type 1/type 2A VWD phenotypes.¹²⁻¹⁵

In this study, we report and characterize a previously undocumented cysteine variant, p.(Cys1084Tyr), that causes a complex, mixed phenotype VWD. We show that loss of this critical cysteine residue differentially associates with qualitative and/or quantitative VWF defects in heterozygous and homozygous individuals causing a variably expressed form of VWD.

Methods

Study approval

Study approval was obtained from the Research Ethics Board of the Hospital for Sick Children, Toronto, Canada, and all study participants gave written informed consent.

Bleeding questionnaires

Bleeding scores were evaluated by the International Society on Thrombosis and Hemostasis Bleeding Assessment Tool for adult family members and the Pediatric Bleeding Questionnaire for pediatric subjects by an expert administrator.^{16,17}

DNA sequencing

EDTA-anticoagulated whole blood was obtained from all family members, and genomic DNA was isolated from leukocytes using the Genra Puregene extraction kit (Qiagen, Germantown, MD, USA). The entire coding region of *VWF* and *F8* of the index case (IC) was sequenced by Sanger methodologies and intron/exon boundaries, the 5' and 3' untranslated regions, and the proximal promoter regions of *F8*. The presence of the novel variant was confirmed via bi-directional sequencing in the IC. Direct sequencing of *VWF* exon 25 was carried out to detect the variant in the additional family members. Sequencing data can be found in GenBank (ncbi.nlm.nih.gov/genbank, accession numbers OM169364, OM169365, and OM169366).

Coagulation studies

VWF:Ag was determined by enzyme-linked immunosorbent assay (ELISA) using polyclonal VWF antibodies A0082 and P0226 (Dako,

Glostrup, Denmark). VWF:GPIbM was measured using the INNOVANCE VWF Ac Assay (Siemens Healthcare Diagnostics, Marburg, Germany), and collagen-binding activity was determined as before.^{18,19} VWF propeptide was measured via an in-house ELISA using monoclonal capture antibodies 239.2 and 239.3 and biotinylated 242.2 and 242.6 for detection. VWF propeptide antibodies were provided by S. Haberichter (Versiti, Blood Center of Wisconsin, Milwaukee, WI). Factor VIII (FVIII):C was measured by 1-stage activated partial thromboplastin time clotting assay using an automated coagulometer (Siemens BCS XP, Oakville, ON, Canada).

Desmopressin challenge

Desmopressin (0.3 µg/kg) was administered IV, and blood was drawn at baseline and 1, 3, and 6 hours after administration. The VWF:Ag, VWF:GPIbM, and FVIII:C responses were plotted as concentration against time, and data were fitted to a mono-exponential curve. The 1-hour time point was taken as the beginning of the elimination phase. Half-lives were calculated from the first-order rate constant (k) for the elimination phase.

Multimer analysis

VWF multimers were analyzed as previously described.²⁰

Expression plasmids and mutagenesis

The VWF expression vectors, pCIneohuVWF for recombinant human VWF protein production, and pSC11ETmVWF for hydrodynamic delivery have previously been described.²⁰ Expression plasmid pCIneohuVWF was used as a template to generate the p.(Cys1084Tyr), p.(Cys1060Ala), and p.(Cys1060Ser) expression plasmids via site-directed mutagenesis using the Q5 Site-Directed Mutagenesis Kit (New England Biolabs, Whitby, ON, Canada). Expression plasmid pCIneohuVWF p.(Cys1084Tyr) was subsequently used as a template to generate p.(Cys1060Ala;Cys1084Tyr) and p.(Cys1060Ser;Cys1084Tyr). Site-directed mutagenesis was also performed on the pSC11ETmVWF expression vector to generate pSC11ETmVWF p.(Cys1084Tyr).

Protein expression studies

HEK 293T cells were transiently transfected with variant or wild-type (WT) *VWF* cDNA via liposomal transfer according to the manufacturer's instructions (Lipofectamine 2000, ThermoFisher Scientific, Carlsbad, CA). Following transfection, cells were grown for 24 hours in Dulbecco's modified Eagle's medium (Life Technologies, Grand Island, NY) with 10% (vol/vol) fetal bovine serum (Wisent Bioproducts, Saint-Jean-Baptiste, QC, Canada) and for a further 48 hours in OptiMEM serum-free medium (Life Technologies, Grand Island, NY). Conditioned media were collected, and secreted VWF was concentrated using Amicon Ultra 0.5-mL 50K molecular weight cut-off centrifugal filter devices (Millipore, Cork, Ireland). VWF:Ag was measured in conditioned medium and in cell lysates by VWF:Ag ELISA.

Animal studies

Animal experiments were approved by the Queen's University Animal Care Committee (Kingston, ON, Canada). VWF^{-/-} mice on a C57Bl/6 background (8-12 weeks) were used. For clearance studies, VWF was administered at 7.5 µg/mouse by tail vein injection. In

vivo VWF expression was induced via hydrodynamic injection of *Vwf* cDNA as previously described.²¹

Immunocytochemistry

Immunocytochemical analysis of transiently transfected HEK 293 was carried out as described previously.²² Imaging was performed using a Leica TCS SP8 confocal microscope (Leica Microsystems, Concord, ON, Canada). Individual cells were imaged through a z-stack (Z-dimension of 2 to 3 μm) acquisition mode using the HC PL APO CS2 63×/1.40 oil objective. Images were deconvolved using Huygens Essential Software (Scientific Volume Imaging, Hilversum, Netherlands) and analyzed using LAS-X Software (Leica Microsystems, Concord, ON, Canada).

Immunohistochemistry

Diaminobenzidine (DAB) peroxidase staining for VWF expression by mouse hepatocytes following hydrodynamic injection was performed on formalin-fixed paraffin-embedded tissue using a rabbit polyclonal antibody (A0082; DAKO, Glostrup, Denmark) on a Ventana Discovery Immunostainer (Ventana Medical System, Tucson, AZ, USA).

Results

Identification of a novel cysteine variant in a consanguineous family with VWD

The IC (III-2) is a 9-year-old girl diagnosed with VWD following episodes of epistaxis requiring medical intervention. Sequencing of the

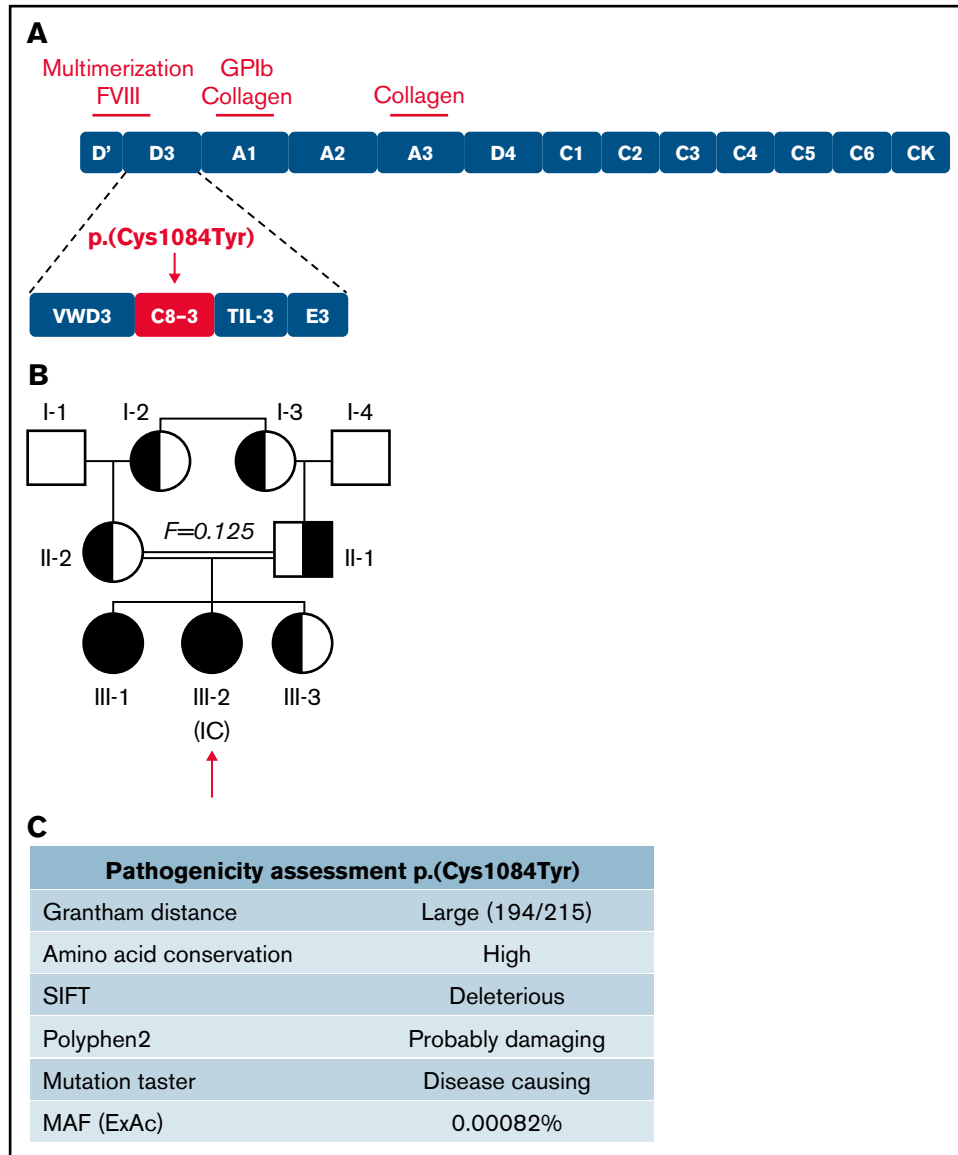


Figure 1. Inheritance and pathogenicity of novel VWF variant p.(Cys1084Tyr). (A) Schematic representation of the VWF domain structure with subdomain architecture and critical functional sites. The location of the p.(Cys1084Tyr) variant in the C8-3 subdomain is shown. (B) Three-generation pedigree of a consanguineous family diagnosed with VWD. Homozygous individuals are represented by black symbols and heterozygous individuals by half-filled symbols. (C) Pathogenicity prediction for VWF variant p.(Cys1084Tyr).

Table 1. Laboratory and clinical phenotypic data for family members heterozygous and homozygous for p.(Cys1084Tyr)

	II-1	II-2	III-1	III-2 (IC)	III-3	Normal range
Sex	M	F	F	F	F	–
Age	35	41	10	9	3	–
Genotype	c.[3251G>A];[=]	c.[3251G>A];[=]	c.[3251G>A];[3251G>A]	c.[3251G>A];[3251G>A]	c.[3251G>A];[=]	–
BAT score	0	8	4	4	0	0-4 (adult), 0-2 (pediatric)
VWF:Ag (IU/mL)	0.94	0.63	0.38	0.23	0.64	0.50-1.50 (IU/mL)
VWF:GPIbM (IU/mL)	0.41	0.32	0.15	0.11	0.29	0.50-1.50 (IU/mL)
VWF:CB (IU/mL)	0.34	0.26	0.13	0.09	0.3	0.50-1.50 (IU/mL)
VWFpp (IU/mL)	1.13	0.84	0.76	0.56	0.91	0.50-1.50 (IU/mL)
FVIII:C (IU/mL)	0.65	0.83	0.10	0.05	0.72	0.50-1.50 (IU/mL)
VWF:GPIbM/VWF:Ag	0.45	0.50	0.40	0.48	0.45	0.75-1.25
VWF:CBA/VWF:Ag	0.38	0.41	0.34	0.40	0.47	0.75-1.25
VWFpp/VWF:Ag	1.26	1.33	2.01	2.47	1.42	–2.2
FVIII:C/VWF:Ag	0.72	1.31	0.25	0.22	1.12	0.75-1.25
Blood Group	A	O	O	O	O	–

VWF gene revealed a G to A transition (c.3251G>A) in exon 25, predicting a cysteine to tyrosine substitution at amino acid 1084 in the C8-3 subdomain of the VWF D'D3 assembly (Figure 1A), for which the IC was homozygous. Three family members, her father, mother, and younger sibling (II-1, II-2, III-3), were found to be heterozygous for the variant. Her older sibling (III-1) was found to be homozygous for the variant. The family pedigree is shown in Figure 1B. In silico analysis (Alamut Visual software; Interactive Biosoftware, version 2.9.0) suggests that this variant is damaging to protein expression and/or function (Figure 1C). Although this variant has not been documented by the European Association for Haemophilia and Allied Disorders VWF variant database, it was identified in 2 heterozygous males in the ThromboGenomics patient cohort.²³ The variant has since been reported to the ClinVar database (<https://www.ncbi.nlm.nih.gov/clinvar/>; accessed 22 March 2021) as a “Variant of Uncertain Significance” with a minor allele frequency of 0.00082%. Two common benign VWF sequence variants were also identified in certain family members (supplemental Tables 1 and 2). No F8 sequence variants were identified in any family members.

Phenotypic characterization of family members with the p.(Cys1084Tyr) variant

Family phenotypic values are outlined in Table 1. For 3 family members, heterozygosity for the p.(Cys1084Tyr) variant was associated with qualitative VWF defects. Normal VWF:Ag levels but significantly reduced VWF:GPIbM (<0.40 IU/mL) and VWF:CB (<0.35 IU/mL) were observed, consistent with a functional VWF defect and a diagnosis of type 2 VWD. Importantly, the clinical severity of the disease was markedly different among the heterozygous family members. Although the variant exhibited variable expressivity in the father (II-1) and the youngest sibling (III-3) who had normal bleeding scores, the mother (II-2) had a positive bleeding score (BS 8). The well-established quantitative effect of ABO blood group on plasma VWF levels likely contributes to the more elevated VWF:Ag levels observed in the father (II-1, blood group A) but does not account for absence of a bleeding diathesis given the qualitative nature of the defect.^{24,25} The prepubescent age (9 years) of the youngest sibling (III-3) may contribute at least in part to her normal bleeding score.

In addition to the qualitative defects, homozygosity for the p.(Cys1084Tyr) variant was further associated with severely reduced plasma FVIII:C (<0.10 IU/mL) and a quantitative VWF defect. Plasma VWF:Ag levels were significantly reduced (<0.40 IU/mL) and FVIII:C/VWF:Ag in line with a diagnosis of type 2N were observed. Additionally, both homozygous siblings had positive bleeding scores. Taken together, the phenotypic data reveal that the p.(Cys1084Tyr) variant causes variable expressivity of a qualitative form of VWD in the heterozygous family members but results in a fully expressed VWD phenotype in the homozygous individuals who exhibit a more complex condition involving both qualitative and quantitative defects.

Reduction of HMWMs in individuals homozygous for p.(Cys1084Tyr)

To distinguish whether the qualitative aspect of the clinical phenotype was consistent with type 2A or type 2M VWD, VWF multimer analysis was performed on patient plasma (Figure 2A). Densitometric analysis revealed a relative reduction in HMWMs compared with normal pooled plasma for both the heterozygous and homozygous family members (Figure 2B). The reduction in HMWMs was most pronounced in the IC (III-2). This aberrant multimer pattern is characteristic of type 2A VWD and reflects the reduced collagen-binding activity observed in both heterozygous and homozygous family members (Table 1).

p.(Cys1084Tyr) VWF is rapidly cleared after desmopressin administration

To investigate the pathogenic mechanisms associated with p.(Cys1084Tyr), VWF:Ag, VWF:GPIbM, and FVIII:C plasma levels were measured in the homozygous siblings after desmopressin administration (Table 2). Although peak postdesmopressin VWF:Ag levels were elevated approximately threefold over baseline and normalized (>0.5 IU/mL) after 1 hour in both cases, the observed increases in plasma VWF:Ag levels were not sustained (Figure 3A-B). VWF:Ag half-lives were significantly reduced compared with the 12- to 18-hour half-life described in healthy individuals and were calculated as 4.20 and 6.41 hours for the IC (III-2) and her sibling (III-1),

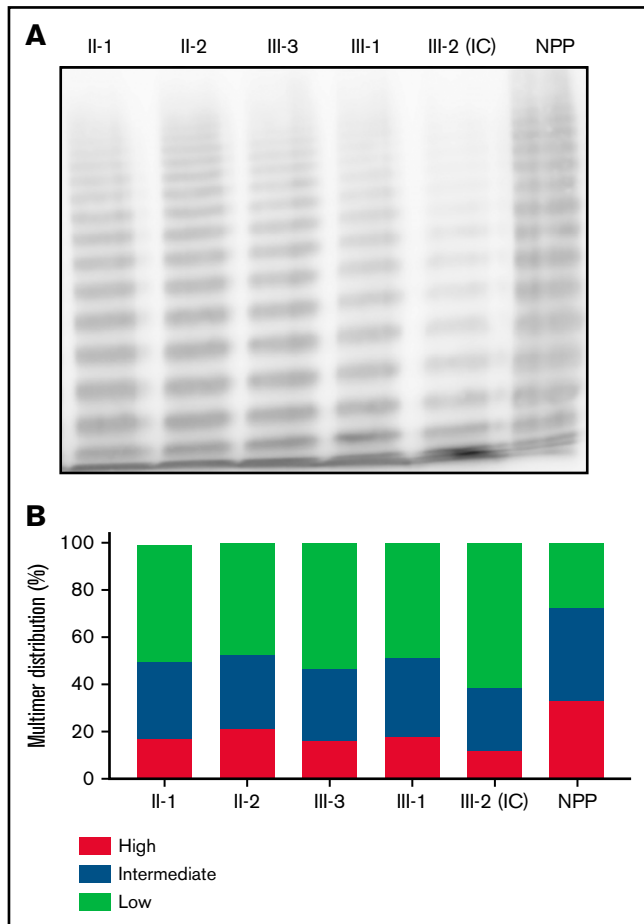


Figure 2. Phenotypic characterization of family members. (A) Multimer distribution of plasma VWF in heterozygous and homozygous family members relative to normal pooled plasma (NPP). Heterozygous and, to a greater degree, homozygous family members show a relative reduction in high molecular weight multimers. (B) Multimer analysis was performed using 1-dimensional densitometry and the relative percentage of high-, intermediate-, and low-molecular-weight multimers was reported. The greatest reduction in high-molecular-weight material was observed in the IC.

respectively.²⁶ Consistently, a marked reduction in postdesmopressin VWF:GPIbM survival was also observed (IC III-2, $t_{1/2}$ 2.40 hours; III-3, $t_{1/2}$ 4.27 hours).

Table 2. Pre- and postdesmopressin clinical laboratory values for homozygous family members

Laboratory values	III-1	III-2 (IC)
Base-line VWF:Ag (IU/mL)	0.26	0.20
Peak VWF:Ag (IU/mL)	0.79	0.67
VWF:Ag half-life (hours)	6.41	4.20
Base-line VWF:GPIbM (IU/mL)	0.16	0.10
Peak VWF:GPIbM (IU/mL)	0.72	0.64
VWF:GPIbM half-life (hours)	4.27	2.40
Base-line FVIII:C (IU/mL)	0.05	0.04
Peak FVIII:C (IU/mL)	0.62	0.61
FVIII:C half-life (IU/mL)	1.90	1.05

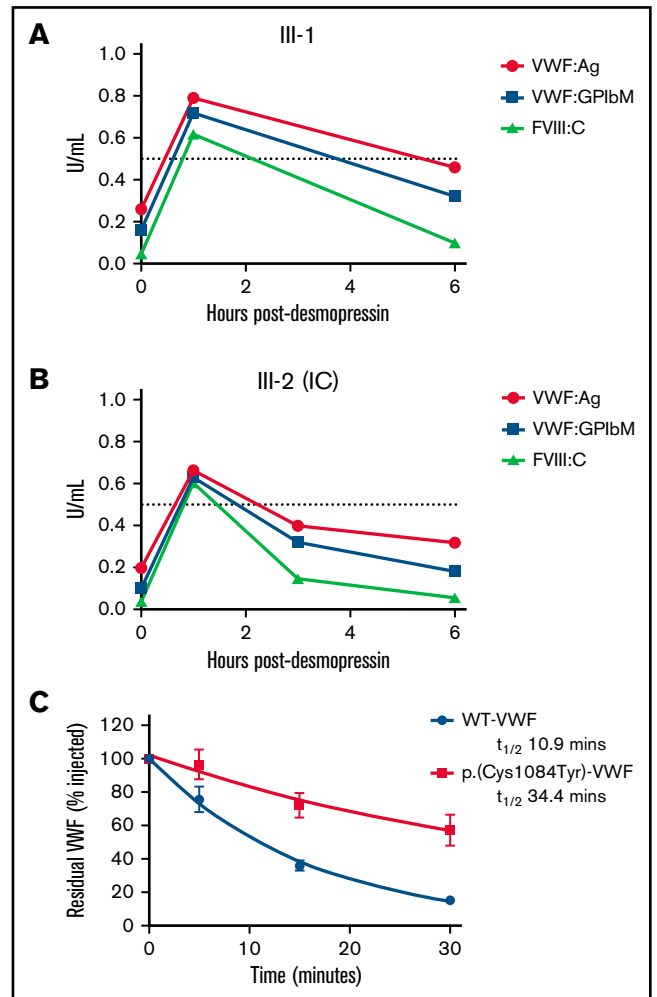


Figure 3. Clearance kinetics of p.(Cys1084Tyr)-VWF. Time course of the postdesmopressin response in siblings III-1 (A) and III-2 (B). Markedly reduced VWF:Ag, VWF:GPIbM and FVIII:C half-lives were observed following the 1-hour peak. The dashed line represents normalized VWF:Ag, VWF:GPIbM and FVIII:C plasma levels (0.5 IU/mL). (C) The influence of p.(Cys1084Tyr) on VWF clearance in a mouse model of VWD. Prolonged survival of p.(Cys1084Tyr)-VWF was observed. Data were fitted to a 1-phase exponential decay ($n = 3$ mice per time point).

Additionally, the relative FVIII:C response was significant (15- and 12-fold increase over baseline for III-2 (IC) and III-1, respectively), and the absolute peak postdesmopressin FVIII:C values were in the normal range. In keeping with the reduced VWF:Ag survival, significantly shortened FVIII:C survival was also apparent (III-2 [IC], $t_{1/2}$ 1.05 hours; III-3, $t_{1/2}$ 1.90 hours). Moreover, the shorter half-life of FVIII:C compared with VWF:Ag confirmed the presence of a FVIII-binding defect in these individuals. Collectively, the desmopressin response kinetics demonstrate that both accelerated VWF clearance and defective FVIII binding contribute to VWD pathophysiology in family members homozygous for the p.(Cys1084Tyr) variant.

Prolonged survival of p.(Cys1084Tyr)-VWF in VWF^{-/-} mice

To investigate the mechanisms underlying rapid clearance of p.(Cys1084Tyr)-VWF, recombinant VWF infusions were carried out in

VWF^{-/-} mice. Surprisingly, the half-life of p.(Cys1084Tyr)-VWF was significantly prolonged compared with WT-VWF ($t_{1/2}$ 34.4 vs 10.9 minutes, respectively; $P < .0001$, Figure 3C). Although human and mouse VWF share ~80% amino acid identity and several cysteine VWF variants have previously been shown to undergo rapid clearance in this mouse model, it is apparent that the rapid clearance of p.Cys1084Tyr-VWF was not recapitulated in this setting.^{13,27} The significance of this finding and the underlying molecular mechanisms remain unclear.

p.(Cys1084Tyr) is associated with reduced VWF secretion and aberrant multimerization in vitro

To assess the impact of the p.(Cys1084Tyr) variant on VWF synthesis and secretion, HEK 293T cells were transiently transfected with full-length human VWF expression vectors encoding WT or the p.(Cys1084Tyr) variant to mimic the heterozygous and homozygous states. For cells transfected with the cDNA coding for the p.(Cys1084Tyr) variant alone, significantly reduced VWF secretion was observed in the conditioned media ($25.2 \pm 7.0\%$ of WT-VWF; $P < .0001$; Figure 4A-B). For cotransfected cells, a less severe reduction in VWF secretion was observed ($58.4 \pm 5.2\%$ of WT-VWF; $P < .0001$), indicating that the p.(Cys1084Tyr) variant negatively affected VWF secretion in a dose-dependent manner.

Multimer analysis of the secreted VWF demonstrated aberrant multimerization for the homozygous state that was significantly more severe than that observed in patient plasma. The complete absence of both HMWMs and intermediate-molecular-weight multimers was observed, with only the lowest-molecular-weight VWF multimers visible (Figure 4C). This phenomenon has previously been reported and likely represents cell-specific differences in the posttranslational and quality control pathways in endothelial vs nonendothelial cells.²⁸

To visualize pseudo-WPB formation, transfections were repeated using HEK 293 cells. Imaging studies revealed that the p.(Cys1084Tyr) variant affects packaging and storage of VWF into pseudo-WPBs (Figure 4D). Cells transfected with WT-VWF formed distinct, cigar-shaped pseudo-WPBs, as did cotransfected cells, whereas cells transfected with the p.(Cys1084Tyr) variant alone displayed both granular and diffuse staining. Furthermore, p.(Cys1084Tyr)-VWF staining overlapped with that of ER marker PDI, suggesting that at least a portion of the mutant subunits were retained within the ER. Colocalization was also observed for cotransfected cells, although to a lesser extent. Taken together, these data demonstrate that packaging and secretion of p.(Cys1084Tyr)-VWF is impaired in both the homozygous and heterozygous states.

p.(Cys1084Tyr) abrogates VWF secretion in a mouse model of VWD

To characterize the in vivo effects of the p.(Cys1084Tyr) substitution, we sought to develop a mouse model of this complex form of VWD. Accordingly, in vivo VWF expression was induced via hydrodynamic tail vein injection of the murine *Vwf* cDNA with or without the variant coding for p.(Cys1084Tyr) in VWF^{-/-} mice.

In keeping with previous reports, variable supraphysiologic VWF expression was observed in the plasma of VWF^{-/-} mice that received WT mouse *Vwf* cDNA (VWF:Ag, 17.5 ± 6.4 U/mL).²⁹ In contrast, no VWF was detectable in the plasma of VWF^{-/-} mice that received mouse *Vwf* cDNA coding for the p.(Cys1084Tyr)

variant (Figure 5A). Plasma VWF propeptide was also undetectable in these mice (data not shown). However, immunohistochemical DAB staining of mouse liver sections revealed robust VWF expression in a population of hepatocytes. Intracellular hepatocyte p.(Cys1084Tyr)-VWF expression was comparable to that observed for WT-VWF, with approximately 5% of hepatocytes expressing WT or variant VWF (Figure 5B). In keeping with our in vitro imaging results, in these transient transgenic in vivo studies, p.(Cys1084Tyr)-VWF was synthesized by mouse hepatocytes but was not efficiently secreted into plasma, suggesting compromised VWF secretion. The absence of detectable plasma VWF in this mouse model of VWD precluded any further investigation of the bleeding phenotype associated with this cysteine variant.

Reduced VWF secretion is caused by loss of the p.(Cys1060)-p.(Cys1084) disulfide bond

Evidence exists that the loss of a disulfide bond because of mutation of a cysteine residue and the subsequent effect on protein folding is of greater consequence to VWF expression than the generation of the associated novel free thiol.¹⁵ In WT-VWF an intra-subunit disulfide bond connects p.(Cys1084) to p.(Cys1060) in the C8-3 subdomain, linking and stabilizing the $\alpha 1$ and $\alpha 3$ helices (Figure 6A-B).⁵ Consequently, in patients with the p.(Cys1084Tyr) variant, p.(Cys1060) is predicted to exist as a free thiol (Figure 6A). To assess the impact of the novel free thiol on VWF secretion, serine (conservative) or alanine (nonconservative) p.(Cys1060;Cys1084) double variants were generated via site-directed mutagenesis. Individual removal of p.(Cys1084) or p.(Cys1060) lead to significant reductions in the amount of VWF detected in conditioned media: p.(Cys1084Tyr), $25.2 \pm 7.0\%$; p.(Cys1060Ala), $37.4 \pm 13.0\%$; p.(Cys1060Ser), $11.5 \pm 2.1\%$ (WT-VWF; $P < .01$; Figure 7A-B). However, elimination of the novel free thiol via simultaneous removal of both p.(Cys1060) and p.(Cys1084) did not rescue VWF secretion: p.(Cys1060A;p-Cys1084Tyr), $19.5 \pm 1.9\%$ and p.(Cys1060S;p.Cys1084Tyr), $15.9 \pm 2.4\%$ (WT-VWF; $P < .0001$).

When transfections were repeated in HEK 293 cells to visualize pseudo-WPB formation, a combination of diffuse and granular VWF staining was observed for the double mutants, indicating impaired VWF packaging (Figure 7D). Considerable variation was also observed in the number of pseudo-WPBs formed per cell by each of the double mutants, although the overall number of pseudo-WPBs formed per cell did not significantly differ to WT-VWF (Figure 7C). Collectively, these data demonstrate that the effects of cysteine mutation on VWF secretion are primarily attributable to errant disulfide connectivity caused by the loss of the disulfide bond and subsequent protein misfolding rather than the presence of a free thiol.

Discussion

In this study, we identified and characterized a novel VWD-causing cysteine variant in the VWF D'D3 assembly: p.(Cys1084Tyr). This cysteine variant was found to cause an unusual, variably expressed, and phenotypically complex form of VWD involving intersecting type 1, type 2A, and type 2N phenotypes. Although VWF cysteine variants are known to contribute to the pathogenesis of both type 1 and type 2 VWD, instances of such phenotypic complexity and variability in a single kindred are rare. Extensive characterization of affected family members revealed that, although both heterozygosity

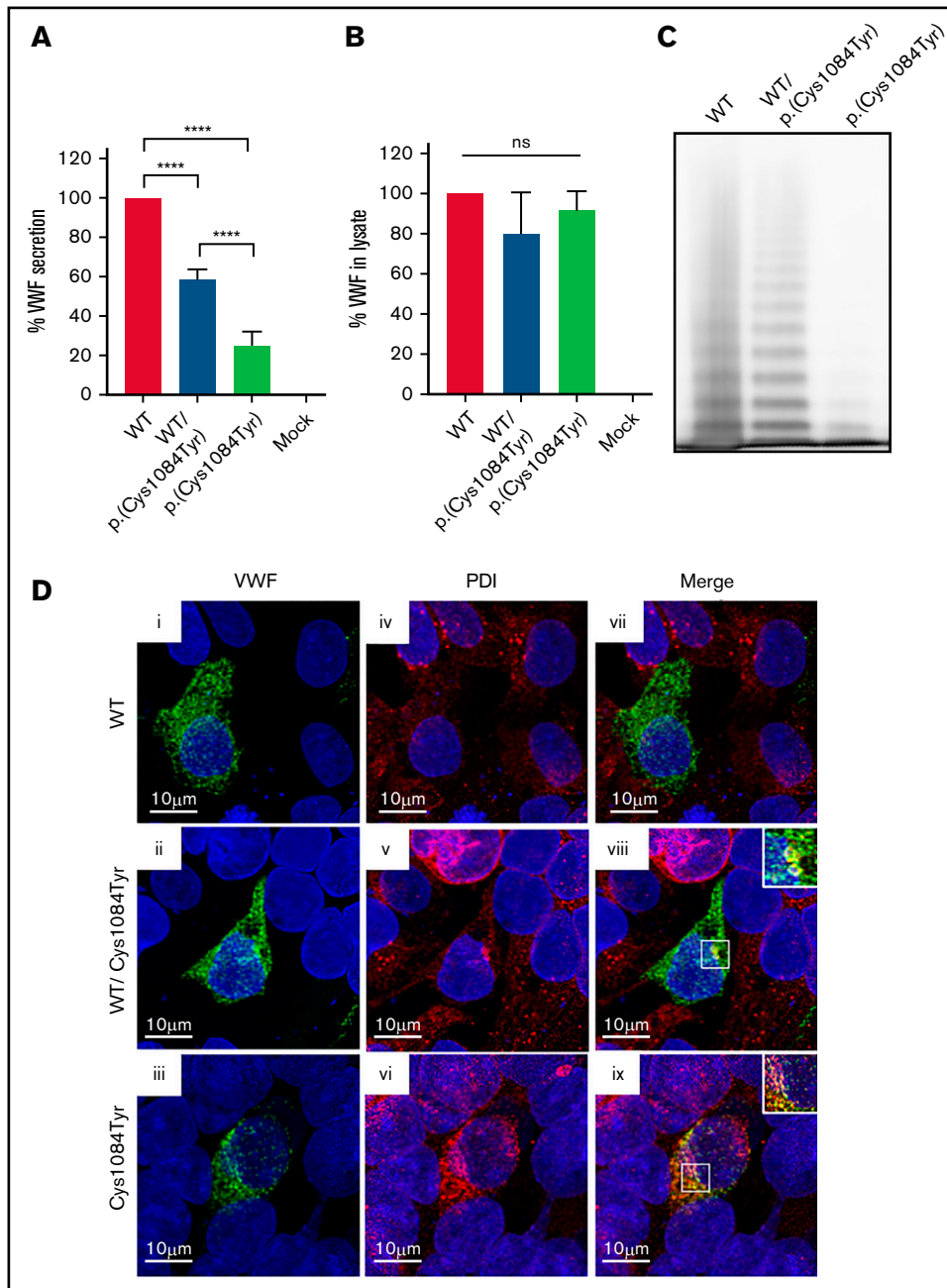


Figure 4. Defective secretion despite normal storage of p.(Cys1084Tyr) VWF in vitro. (A) HEK293T cells were transiently transfected with cDNA encoding WT-VWF, the p.(Cys1084Tyr) variant, or a 1:1 molar ratio of both constructs to mimic the heterozygous state. Transfection with cDNA encoding the p.(Cys1084Tyr) variant led to a significant reduction in the amount of VWF secreted into the conditioned media whether transfected alone or cotransfected with the cDNA coding for WT-VWF. The reduction in VWF secretion was more severe for the transfection mimicking the homozygous condition. Data are represented as mean \pm standard error of the mean (SEM), **** $P < .0001$. (B) No increase in variant VWF was observed in the cellular lysate for either the heterozygous or homozygous state indicating that the p.(Cys1084Tyr) variant does not cause intracellular retention of VWF. (C) Multimer analysis of recombinant VWF showed a relative reduction in high-molecular-weight multimers for VWF produced via cotransfection and a complete absence of high- and intermediate-weight multimers for p.(Cys1084Tyr) VWF. (D) Pseudo-WPB formation was assessed via transient transfection in HEK293 cells. Transfected cells were fixed and stained for VWF (green; i, ii, iii) and resident ER protein protein disulfide isomerase (PDI) (red; iv, v, vi). Merged images (vii, viii, ix) are shown in the final column. For all images, blue indicates 4',6-diamidino-2-phenylindole. Colocalization of VWF and PDI was observed for cotransfected cells (viii) and for cells transfected with p.(Cys1084Tyr)-VWF alone (ix). Magnified views of regions of colocalization are shown in the inset. Images are representative of $n = 3$ independent experiments.

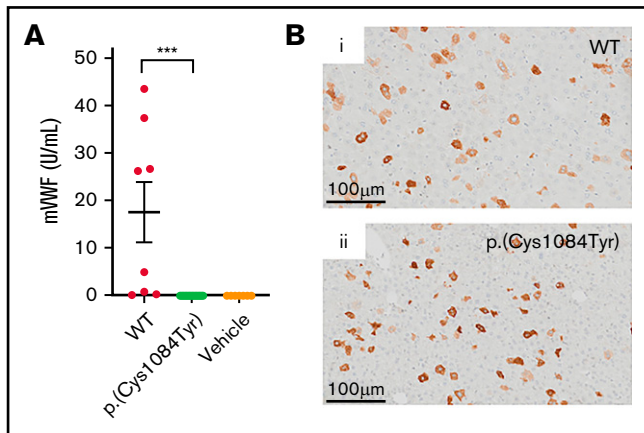


Figure 5. Hepatic expression of p.(Cys1084Tyr) abolishes VWF secretion in $VWF^{-/-}$ mice. (A) Following hydrodynamic gene transfer of the cysteine variant mouse *Vwf* cDNA, no p.(Cys1084Tyr) VWF was detectable in the plasma of $VWF^{-/-}$ mice. Data represent mean \pm SEM, *** $P < .001$. (B) DAB peroxidase staining of formalin-fixed paraffin-embedded mouse liver sections showed equivalent intracellular expression of both WT-VWF and p.(Cys1084Tyr) VWF in $\sim 5\%$ of hepatocytes.

and homozygosity for the p.(Cys1084Tyr) variant were associated with clinical bleeding, they were in fact associated with remarkably dissimilar diagnoses. Based on the recent American Society of Hematology/International Society on Thrombosis and Hemostasis/National Hemophilia Foundation/World Federation of Hemophilia VWD diagnostic criteria, family members who were heterozygous for the cysteine variant were diagnosed with type 2A VWD, whereas homozygous family members displayed a more severe and complex type 1/type 2A/type 2N phenotype.³⁰ Unusually, clinical phenotypic variability was evident not only between homozygous and heterozygous family members but also among the heterozygous (type 2A) family members. Although the mechanistic complexity of type 2A VWD has been documented, with a number of variably influential defects collectively resulting in the overall disease phenotype, type 2A VWD is typically associated with largely consistent expressivity of specific VWF variants.³¹ In this family, however, the mother, who experienced the most severe bleeding symptoms (BS 8), exhibited a compromised VWF:GPIIb/IIIa:Ag and a relative reduction in HMWMs, whereas the father, who had a comparable reduction in VWF:GPIIb/IIIa:Ag and an equivalent multimerization defect, had a normal bleeding score. The reason for this disparity is unclear. However, previous studies have attributed phenotypic variability in type 2 VWD to the variable multimer composition of circulating plasma VWF.³² Consequently, the extent of

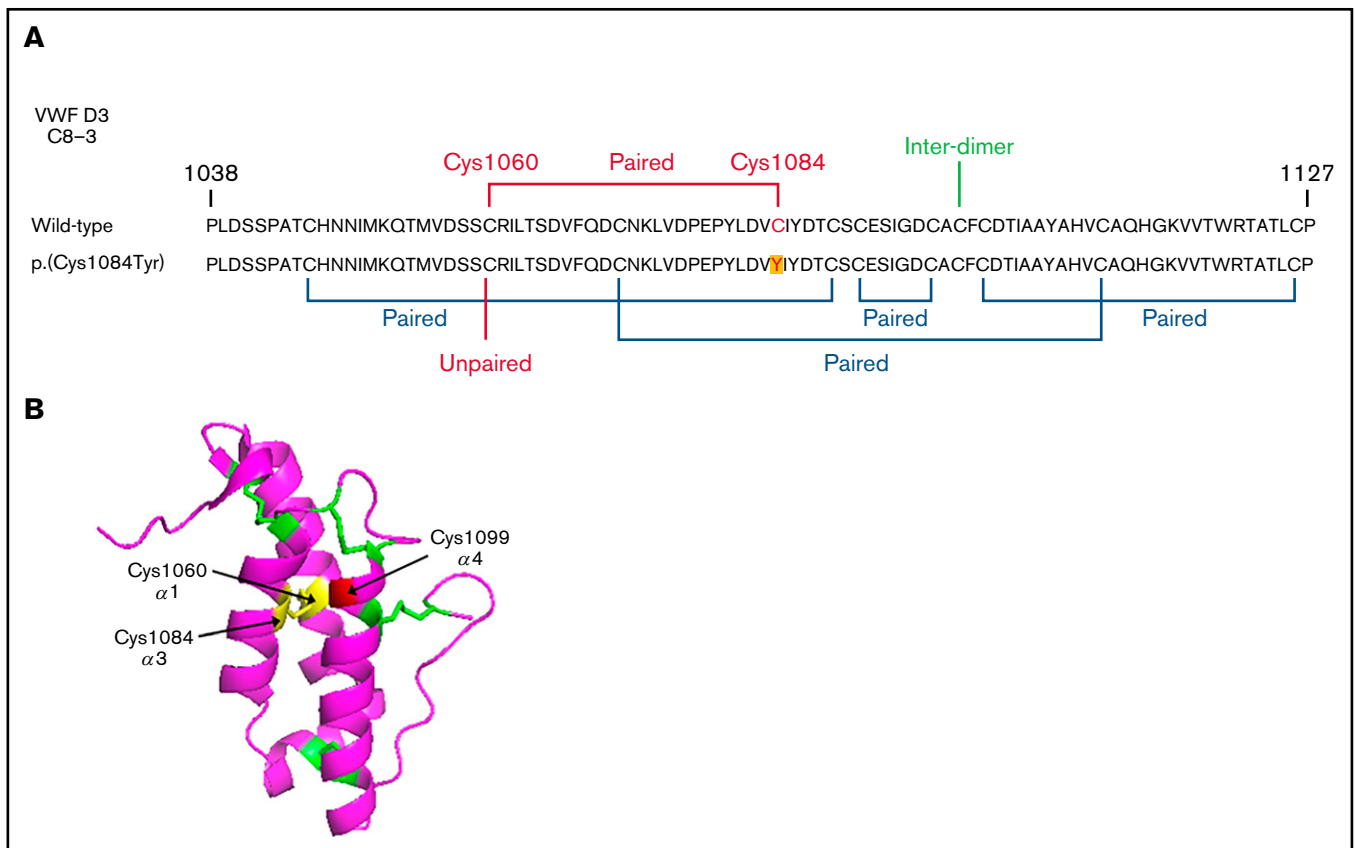


Figure 6. Disulfide connectivity and structural architecture of the VWF C8-3 subunit. (A) Disulfide connectivity of the C8-3 subdomain of the VWF D¹D3 assembly. (B) Location of p.(Cys1084) in the crystal structure of the VWF C8-3 subdomain. Intra-subdomain disulfide bonds are annotated in green, the p.(Cys1060)-p.(Cys1084) disulfide bond in yellow, and the cysteine involved in inter-subunit bonding p.(Cys1099) in red. Protein Data Bank 6N29, accessed 20 March 2021. Image rendering was performed with PyMOL software (version 2.1.1).

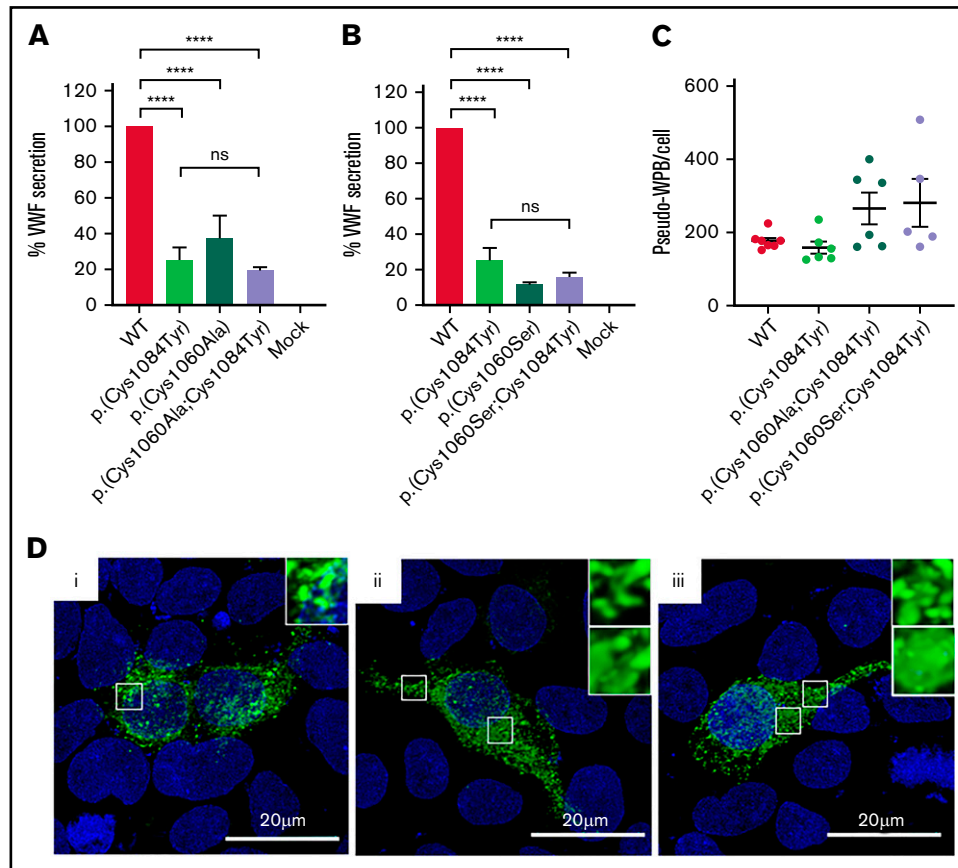


Figure 7. Altered disulfide connectivity because of loss of the p.(Cys1060)-p.(Cys1084) disulfide bond causes reduced VWF secretion. (A) Transient transfection of HEK293 cells with the expression vector encoding p.(Cys1060Ala) caused a significant reduction in VWF secretion. Transfection of cells with the expression vector coding for the p.(Cys1060Ala;Cys1084Tyr) double variant did not rescue VWF secretion. (B) Similar results were observed for p.(Cys1060Ser) and the p.(Cys1060Ser;Cys1084Tyr) double variant. Data are represented as mean \pm SEM, **** $P < .0001$. (C) Three-dimensional quantification of the number of pseudo-WPB/cell revealed no significant difference in the number of storage organelles formed/cell by each variant. (D) Immunofluorescent imaging of WT-VWF (i), p.(Cys1060Ala;Cys1084Tyr) (ii), and p.(Cys1060Ser;Cys1084Tyr) (iii). VWF is depicted in green, and blue represents 4',6-diamidino-2-phenylindole. Elongated rod-shaped WPBs are shown (inset, top). Areas of diffuse VWF staining for p.(Cys1060Ala;Cys1084Tyr) and p.(Cys1060Ser;Cys1084Tyr) indicating impaired regulated storage are also shown (inset, bottom). Images are representative of $n = 3$ independent experiments.

p.(Cys1084Tyr) monomer incorporation into the final circulating multimer of plasma VWF may contribute to the variable expressivity observed in the heterozygous family members.

The detrimental effect of substituting cysteine residues involved in VWF dimerization or multimerization is intuitive. However, the outcomes associated with substitution of other VWF cysteine residues are less predictable, as specific roles for most disulfides in maintaining VWF structure/function have not been definitively determined. The recent resolution of the VWF D'D3 crystal structure has enabled better prediction of these outcomes and provides valuable insight into some of the molecular mechanisms by which variants such as the p.(Cys1084Tyr) substitution cause VWD.⁵

The location of the p.(Cys1060)-p.(Cys1084) disulfide bond within 1 of the 2 noncontiguous FVIII binding sites, as well as its close proximity to p.(Cys1099), a critical residue for VWF multimerization, reveals the mechanistic basis by which p.(Cys1084Tyr) can impact both FVIII binding and VWF multimerization (and thus Gplb and collagen binding).^{5,33} However, the mechanisms governing accelerated clearance of p.(Cys1084Tyr)-VWF are not

readily apparent from examination of the crystal structure. Although pathologic clearance has previously been reported for several cysteine variants in the VWF D3 domain, a detailed understanding of the underlying process has not been resolved.¹³ However, it seems plausible that rapid clearance of these variants involves a common mechanism of conformational distortion caused by the loss of key structural cysteine residues with subsequent exposure of otherwise cryptic clearance receptor-interactive sites. Interestingly, unlike other D3 domain cysteine variants, the standard mouse model of VWF clearance has not proven informative in the context of the p.Cys1084Tyr variant.¹³ However, given the high degree of amino acid identity between the human and murine VWF D'D3 assemblies ($\sim 89\%$) and between the smaller C8-3 subdomains ($\sim 91\%$), it is likely that differences between murine and human forms of key VWF clearance receptors are responsible for the discordant p.Cys1084Tyr clearance profiles. To date, several limitations of the standard mouse model of VWF clearance have been acknowledged. For example, in humans, differential VWF clearance based on ABO(H) blood group status is well documented.^{25,34,35} However, following infusion of blood

group-specific human VWF, this differential ABO(H) effect is not observed in mice.³⁶ In addition, murine scavenger receptor stabilin-2 has been shown to function as a clearance receptor for human but not murine VWF.²² Conversely, murine stabilin-2 clears murine but not human VWF propeptide.³⁷ The mechanistic basis for this is not currently understood but emphasizes the complex, multifactorial nature of VWF clearance and the clear differences between VWF clearance pathways in humans and mice.

Another aspect of the multifaceted phenotype that cannot be further elucidated by examination of the D'D3 crystal structure is the impact of the p.(Cys1084Tyr) variant on VWF secretion. We demonstrated impaired secretion of the p.(Cys1084Tyr) variant both in vitro and in vivo using a heterologous expression system and a transient transgenic mouse model. Notwithstanding this observation, the magnitude of the postdesmopressin response in homozygous individuals provides evidence for the presence of a releasable VWF pool. Taken together, these data suggest that the p.(Cys1084Tyr) variant does not affect stimulated VWF secretion; rather, p.(Cys1084Tyr)-VWF has adverse effects on unstimulated VWF secretion. Unstimulated VWF secretion refers to 2 different secretory pathways: the basal and constitutive VWF secretory pathways. Basal secretion refers to the spontaneous release of VWF from regulated storage in WPBs in the absence of stimulation, whereas constitutive secretion refers to the continuous transfer of nascent VWF from the Golgi network to the outside surface of the cell. Because the current consensus advises that the majority (~80%) of plasma VWF arises from basal secretion from WPBs, and the p.(Cys1084Tyr) variants impairs packing of VWF into these specialized organelles, the question arises if basal but not regulated release of this particular cysteine variant could be compromised, leading to the reduced VWF plasma levels observed in affected individuals.³⁸

We further extended our observations regarding p.(Cys1084Tyr)-VWF secretion to demonstrate that impaired secretion resulted from the loss of the disulfide bond rather than the presence of the novel free thiol. Importantly, however, this does not negate the possibility that the presence of the free thiol may contribute to other aspects of the complex phenotype. Variants at both p.(Cys1060) and p.(Cys1084) have been reported to cause VWD.¹¹ Although homozygosity for p.(Cys1084Tyr) is associated with the complex mixed phenotype described herein, previous reports have described type 2N VWD in a patient homozygous for p.(Cys1060Arg).³⁹ Homozygous loss of p.(Cys1060) was associated with a dramatic reduction in FVIII-binding ability and a relative loss of HMWMs. However, VWF:Ag and VWF:RCo were normal. In light of the observation that both cases of VWD are associated with the disruption of the same intra-subunit disulfide bond, it is possible that the phenotypic differences observed for p.(Cys1060Arg) and p.(Cys1084Tyr) may reflect the relative proximity of the novel free thiol to, and potential interference with, critical functional sites (Figure 6A-B). Differential disulfide rearrangements arising from p.(Cys1084Tyr) vs p.(Cys1060Arg) may also have more profound effects on VWF structure and function.

The data herein serve to highlight the previously underappreciated complexities of cysteine variant VWD. Importantly, our study also provides insight into the limitations of the VWD classification system. Under the current VWD classification criteria, the heterozygous and homozygous members of this family are differentially categorized. The heterozygous family members are easily classified; however, the phenotypic classification of the homozygous individuals proves more difficult. At present, no definitive guidance exists on the appropriate classification of mixed phenotype forms of VWD. Thus, the questions arise as to whether this should be based on the most dominant phenotype, whether this can be unambiguously established in every case, and whether effective clinical management requires absolute classification of the disease. As our understanding of VWF biology continues to evolve, so too will the complexity of classifying the condition based on discrete phenotypes.

Acknowledgments

The authors thank G. Jones and S. Tinlin of the National Inherited Bleeding Disorder Genotyping Laboratory, L. Boudreau and S. Virk of Queen's Laboratory for Molecular Pathology, and P. Lima from Queen's CardioPulmonary Unit for technical assistance.

The study was supported by a foundation grant from the Canadian Institutes of Health Research (FDN154285). D.L. is the recipient of a Canada Research Chair in Molecular Hemostasis.

Authorship

Contribution: O.R. and L.L.S. designed and performed experiments and interpreted results; C.B. and K.N. performed experiments; O.R. wrote the manuscript; L.L.S., D.L., and P.D.J. edited the manuscript; M.R. performed the expert-administered BAT; and R.K., M.R., T.H., and M.D.C. recruited study subjects and performed sample collection.

Conflict-of-interest disclosure: O.R. has received research funding and honoraria for participating on advisory boards for CSL Behring. P.D.J. receives research funding from Bayer, Takeda and CSL Behring. M.D.C. has received research support from Bayer, Bioverativ/Sanofi, CSL-Behring, Novo Nordisk, Octapharma, Pfizer, and Shire and has received honoraria for speaking/participating on advisory boards for Bayer, Bioverativ/Sanofi, Biotest, CSL Behring, Grifols, LFB, Novo Nordisk, Octapharma, Pfizer, Roche, and Shire. D.L. has received research funding from Shire, Bayer, Bioverativ, CSL Behring, and Octapharma. The remaining authors declare no competing financial interests.

ORCID profiles: R.K., 0000-0002-6913-2808; P.D.J., 0000-0003-4649-9014; M.D.C., 0000-0001-5350-1763.

Correspondence: David Lillicrap, Richardson Laboratory, Queen's University, 88 Stuart Street, Kingston, ON K7L 3N6; e-mail: david.lillicrap@queensu.ca.

References

1. Zhou YF, Eng ET, Zhu J, Lu C, Walz T, Springer TA. Sequence and structure relationships within von Willebrand factor. *Blood*. 2012;120(2):449-458.
2. Choi H, Aboufatova K, Pownall HJ, Cook R, Dong JF. Shear-induced disulfide bond formation regulates adhesion activity of von Willebrand factor. *J Biol Chem*. 2007;282(49):35604-35611.
3. Ganderton T, Wong JWH, Schroeder C, Hogg PJ. Lateral self-association of VWF involves the Cys2431-Cys2453 disulfide/dithiol in the C2 domain. *Blood*. 2011;118(19):5312-5318.
4. Shapiro SE, Nowak AA, Wooding C, Birdsey G, Laffan MA, McKinnon TAJ. The von Willebrand factor predicted unpaired cysteines are essential for secretion. *J Thromb Haemost*. 2014;12(2):246-254.
5. Dong X, Leksa NC, Chhabra ES, et al. The von Willebrand factor D'D3 assembly and structural principles for factor VIII binding and concatamer biogenesis. *Blood*. 2019;133(14):1523-1533.
6. Cruz MA, Handin RI, Wise RJ. The interaction of the von Willebrand factor-A1 domain with platelet glycoprotein Ib/IX. The role of glycosylation and disulfide bonding in a monomeric recombinant A1 domain protein. *J Biol Chem*. 1993;268(28):21238-21245.
7. Butera D, Passam F, Ju L, et al. Autoregulation of von Willebrand factor function by a disulfide bond switch. *Sci Adv*. 2018;4(2):EAAQ1477.
8. Luken BM, Winn LYN, Emsley J, Lane DA, Crawley JTB. The importance of vicinal cysteines, C1669 and C1670, for von Willebrand factor A2 domain function. *Blood*. 2010;115(23):4910-4913.
9. Goodeve A, Eikenboom J, Castaman G, et al. Phenotype and genotype of a cohort of families historically diagnosed with type 1 von Willebrand disease in the European study, Molecular and Clinical Markers for the Diagnosis and Management of Type 1 von Willebrand Disease (MCMDM-1VWD). *Blood*. 2007;109(1):112-121.
10. James PD, Notley C, Hegadorn C, et al. The mutational spectrum of type 1 von Willebrand disease: results from a Canadian cohort study. *Blood*. 2007;109(1):145-154.
11. University of Sheffield. ISTH SSC VWF Database. <http://www.vwf.group.shef.ac.uk/index.html>. Accessed 24 June 2021.
12. Eikenboom JC, Matsushita T, Reitsma PH, et al. Dominant type 1 von Willebrand disease caused by mutated cysteine residues in the D3 domain of von Willebrand factor. *Blood*. 1996;88(7):2433-2441.
13. Schooten CJ, Tjernberg P, Westein E, et al. Cysteine-mutations in von Willebrand factor associated with increased clearance. *J Thromb Haemost*. 2005;3(10):2228-2237.
14. Gadisseur A, Berneman Z, Schroyens W, Michiels JJ. Laboratory diagnosis of von Willebrand disease type 1/2E (2A subtype IIE), type 1 Vicenza and mild type 1 caused by mutations in the D3, D4, B1-B3 and C1-C2 domains of the von Willebrand factor gene. Role of von Willebrand factor multimers and the von Willebrand factor propeptide/antigen ratio. *Acta Haematol*. 2009;121(2-3):128-138.
15. Bodó I, Katsumi A, Tuley EA, Eikenboom JCJ, Dong Z, Sadler JE. Type 1 von Willebrand disease mutation Cys1149Arg causes intracellular retention and degradation of heterodimers: a possible general mechanism for dominant mutations of oligomeric proteins. *Blood*. 2001;98(10):2973-2979.
16. Rodeghiero F, Tosetto A, Abshire T, et al; ISTH/SSC joint VWF and Perinatal/Pediatric Hemostasis Subcommittees Working Group. ISTH/SSC bleeding assessment tool: a standardized questionnaire and a proposal for a new bleeding score for inherited bleeding disorders. *J Thromb Haemost*. 2010;8(9):2063-2065.
17. Bowman M, Riddel J, Rand ML, Tosetto A, Silva M, James PD. Evaluation of the diagnostic utility for von Willebrand disease of a pediatric bleeding questionnaire. *J Thromb Haemost*. 2009;7(8):1418-1421.
18. Ni Y, Nesrallah J, Agnew M, Geske FJ, Favalaro EJ. Establishment and characterization of a new and stable collagen-binding assay for the assessment of von Willebrand factor activity. *Int J Lab Hematol*. 2013;35(2):170-176.
19. Favalaro EJ, Mohammed S. Towards improved diagnosis of von Willebrand disease: comparative evaluations of several automated von Willebrand factor antigen and activity assays. *Thromb Res*. 2014;134(6):1292-1300.
20. Pruss CM, Golder M, Bryant A, et al. Pathologic mechanisms of type 1 VWD mutations R1205H and Y1584C through in vitro and in vivo mouse models. *Blood*. 2011;117(16):4358-4366.
21. Golder M, Pruss CM, Hegadorn C, et al. Mutation-specific hemostatic variability in mice expressing common type 2B von Willebrand disease substitutions. *Blood*. 2010;115(23):4862-4869.
22. Swystun LL, Lai JD, Notley C, et al. The endothelial cell receptor stabilin-2 regulates VWF-FVIII complex half-life and immunogenicity. *J Clin Invest*. 2018;128(9):4057-4073.
23. Downes K, Megy K, Duarte D, et al; NIHR BioResource. Diagnostic high-throughput sequencing of 2396 patients with bleeding, thrombotic, and platelet disorders. *Blood*. 2019;134(23):2082-2091.
24. O'Donnell JS, McKinnon TAJ, Crawley JTB, Lane DA, Laffan MA. Bombay phenotype is associated with reduced plasma-VWF levels and an increased susceptibility to ADAMTS13 proteolysis. *Blood*. 2005;106(6):1988-1991.
25. Gallinaro L, Cattini MG, Sztukowska M, et al. A shorter von Willebrand factor survival in O blood group subjects explains how ABO determinants influence plasma von Willebrand factor. *Blood*. 2008;111(7):3540-3545.
26. Borchiellini A, Fijnvandraat K, ten Cate JW, et al. Quantitative analysis of von Willebrand factor propeptide release in vivo: effect of experimental endotoxemia and administration of 1-deamino-8-D-arginine vasopressin in humans. *Blood*. 1996;88(8):2951-2958.

27. Rawley O, O'Sullivan JM, Chion A, et al. von Willebrand factor arginine 1205 substitution results in accelerated macrophage-dependent clearance in vivo. *J Thromb Haemost.* 2015;13(5):821-826.
28. Haberichter SL, Budde U, Obser T, Schneppenheim S, Wermes C, Schneppenheim R. The mutation N528S in the von Willebrand factor (VWF) propeptide causes defective multimerization and storage of VWF. *Blood.* 2010;115(22):4580-4587.
29. Pergolizzi RG, Jin G, Chan D, et al. Correction of a murine model of von Willebrand disease by gene transfer. *Blood.* 2006;108(3):862-869.
30. James PD, Connell NT, Ameer B, et al. ASH ISTH NHF WFH 2021 guidelines on the diagnosis of von Willebrand disease. *Blood Adv.* 2021;5(1):280-300.
31. Jacobi PM, Gill JC, Flood VH, Jakab DA, Friedman KD, Haberichter SL. Intersection of mechanisms of type 2A VWD through defects in VWF multimerization, secretion, ADAMTS-13 susceptibility, and regulated storage. *Blood.* 2012;119(19):4543-4553.
32. Chen J, Hinckley JD, Haberichter S, et al. Variable content of von Willebrand factor mutant monomer drives the phenotypic variability in a family with von Willebrand disease. *Blood.* 2015;126(2):262-269.
33. Purvis AR, Gross J, Dang LT, et al. Two Cys residues essential for von Willebrand factor multimer assembly in the Golgi. *Proc Natl Acad Sci USA.* 2007;104(40):15647-15652.
34. Albáñez S, Ogiwara K, Michels A, et al. Aging and ABO blood type influence von Willebrand factor and factor VIII levels through interrelated mechanisms. *J Thromb Haemost.* 2016;14(5):953-963.
35. Haberichter SL, Balistreri M, Christopherson P, et al. Assay of the von Willebrand factor (VWF) propeptide to identify patients with type 1 von Willebrand disease with decreased VWF survival. *Blood.* 2006;108(10):3344-3351.
36. Groeneveld DJ, van Bekkum T, Cheung KL, et al. No evidence for a direct effect of von Willebrand factor's ABH blood group antigens on von Willebrand factor clearance. *J Thromb Haemost.* 2015;13(4):592-600.
37. Rawley O, Brown C, Dwyer C, Nesbitt K. Clearance of mouse VWF propeptide is mediated by stabilin-2 and is regulated by N-linked glycan expression. *Res Pract Thromb Haemost.* 2018;2(suppl 1):1-368.
38. Gibling JP, Hewlett LJ, Hannah MJ. Basal secretion of von Willebrand factor from human endothelial cells. *Blood.* 2008;112(4):957-964.
39. Hilbert L, Jorieux S, Proulle V, et al; INSERM Network on Molecular Abnormalities in von Willebrand Disease. Two novel mutations, Q1053H and C1060R, located in the D3 domain of von Willebrand factor, are responsible for decreased FVIII-binding capacity. *Br J Haematol.* 2003;120(4):627-632.